CONF-9606158--1

THE EFFECT OF THERMAL AGING ON THE THERMAL CONDUCTIVITY OF PLASMA SPRAYED AND EB-PVD THERMAL BARRIER COATINGS

Ralph B. Dinwiddie, Stephen C. Beecher and Wallace D. Porter
High Temperature Materials Laboratory
Oak Ridge National Laboratory
Oak Ridge, TN 37831-6064

Ben A. Nagaraj
G.E. Aircraft Engines
Mail Drop H85
Cincinnati, OH 45215

ABSTRACT

Thermal barrier coatings (TBCs) applied to the hot gas components of turbine engines lead to enhanced fuel efficiency and component reliability. Understanding the mechanisms which control the thermal transport behavior of the TBCs is of primary importance. Electron beam-physical vapor deposition (EB-PVD) and air plasma spraying (APS) are the two most commonly used coating techniques. These techniques produce coatings with unique microstructures which control their performance and stability. The density of the APS coatings was controlled by varying the spray parameters. The low density APS yttria-partially stabilized zirconia (yttria-PSZ) coatings yielded a thermal conductivity that is lower than both the high density APS coatings and the EB-PVD coatings. The thermal aging of both fully and partially stabilized zirconia are compared. The thermal conductivity of the coatings permanently increases upon exposure to high temperatures. These increases are attributed to microstructural changes within the coatings. This increase in thermal conductivity can be modeled using a relationship which depends on both the temperature and time of exposure. Although the EB-PVD coatings are less susceptible to thermal aging effects, results suggest that they typically have a higher thermal conductivity than APS coatings before thermal aging. The increases in thermal conductivity due to thermal aging for plasma sprayed partially stabilized zirconia have been found to be less than for plasma sprayed fully stabilized zirconia coatings.

NOMENCLATURE

APS = atmospheric plasma spray
α = thermal diffusivity, cm^2/s
Cp = specific heat, J/kg K
EB-PVD = electron beam-physical vapor deposition
FSZ = fully stabilized zirconia
HTML = High Temperature Materials Laboratory
K = thermal conductivity after heat treatment, W/m K
K_O = as-fabricated thermal conductivity, W/m K
L-M = Larson-Miller parameter as given in Eq. 2 below
ORNL = Oak Ridge National Laboratory
PSZ = partially stabilized zirconia
ρ = bulk density, g/cm^3
T = absolute temperature, Kelvin
TBC = thermal barrier coating

INTRODUCTION

The drive for increased gas turbine engine thrust and fuel efficiency has resulted in a continuous increase in hot section temperatures. Several generations of superalloys and cooling schemes have been developed over the past 20 years to make these increases in turbine inlet temperatures possible. However, the limits of stress rupture, surface protection, and melting point make these improvements increasingly difficult. Thermal barrier coatings (TBCs) can be used to increase lives of hot section components. Alternatively, TBCs can be used to increase the engine efficiency by increasing the operating temperatures or by reducing the amount of cooling air to maintain the same alloy temperatures. Current turbine airfoil cooling technology can reduce the average metal temperature by 111-167°C (200-300°F) with a 250 micrometer (10 mil) thick TBC (Meier, and Gupta, 1992). Using the same thickness of TBC, the temperature difference across the TBC can be increased or decreased by varying the amount of cooling air passing through the internal passages of airfoils. For the same cooling design of the airfoil, the temperature difference across the TBC

DISCLAIMER

is directly proportional to the thermal conductivity of the TBC (all other parameters being equal).

TBCs have been used extensively since the mid 1970s for life extension of combustor and afterburner components. Plasma sprayed zirconia with approximately 7 weight % yttria for partial stabilization of the tetragonal phase was determined to be the most successful approach for these applications. The combination of very low thermal conductivity, high melting point, chemical inertness (Wortman, B.A.Nagaraj, 1989), and a relatively high coefficient of thermal expansion has made zirconia an ideal material for a TBC.

Two types of thermal barrier coatings have been developed for aircraft engine use: plasma spray and EB-PVD. Numerous versions of plasma spray TBCs have been used successfully on a wide range of components. The initial applications were in the combustor and afterburner where atmospheric plasma spray (APS) bond coats of NiCrAlY with a porous 7% yttria-PSZ top coat were successful. In the late 1980s, plasma spray TBCs were introduced to stationary nozzle components in the turbine. Here, higher temperatures forced the use of low pressure plasma spray MCrAlY bond coats for improved oxidation protection and longer life. Also in the late 1980s, EB-PVD TBCs were developed to the point where production of both turbine blades and vanes was practical.

In the plasma spray coating process (see Fig. 1), molten or semi-molten particles deposit as splats. In the EB-PVD coating process (see Fig. 2), gaseous molecules of yttria and zirconia

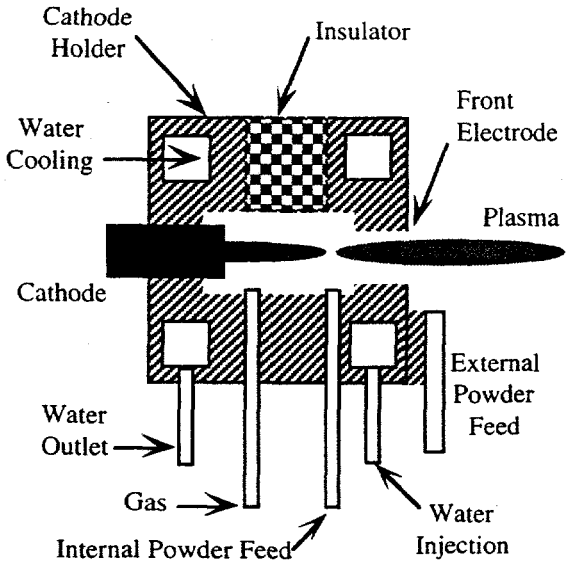

Fig. 1. Typical Plasma Spray Gun.

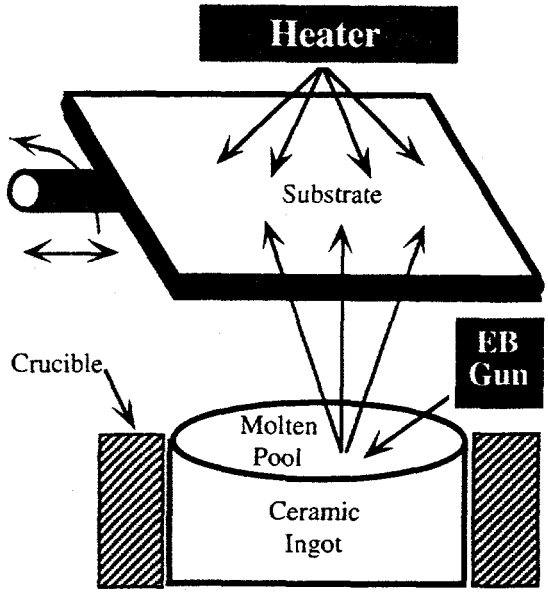

Fig. 2. Typical EB-PVD Coater.

deposit directly on the substrate (opposite of sublimation). The EB-PVD coatings typically have a columnar microstructure, with continuous vertical porosity between the columns, as shown in Fig. 3. In addition, EB-PVD TBCs also have micropores within the columns corresponding to each rotation of the specimen (or part) over the pool. Figure 4 shows a typical plasma sprayed coating which has more horizontal porosity along splat lines. The amount and morphology of the porosity influences the thermal insulation provided by the TBC (Eaton et al., 1994).

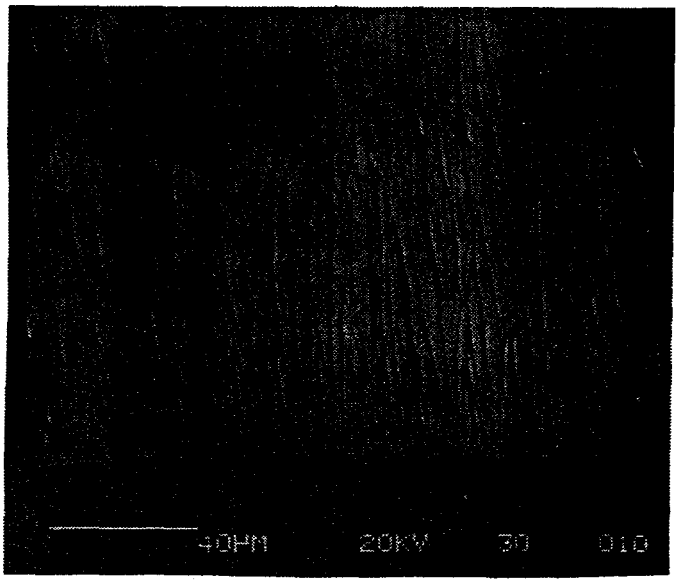

Fig. 3. Typical EB-PVD Microstructure.

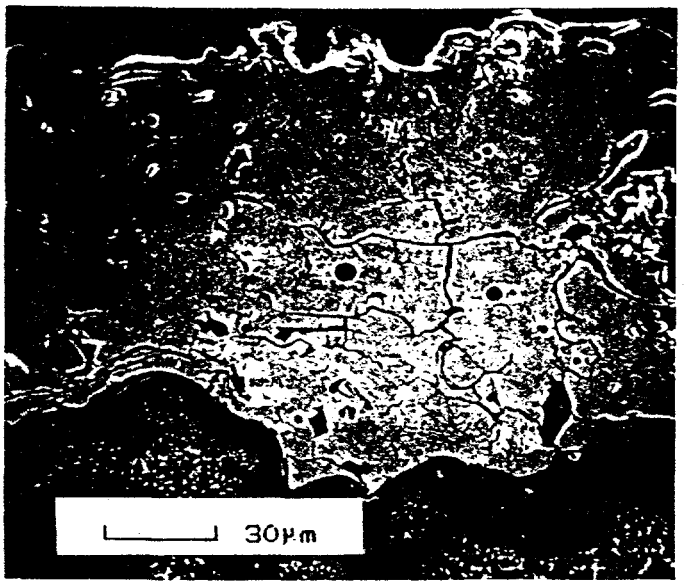

Fig. 4. Typical Plasma Sprayed Microstructure.

Generally, the greater the amount of porosity in the TBC, the lower its thermal conductivity (Taylor, 1992). The level of porosity can be controlled by plasma spray process parameters. Typical parameters affecting the porosity are the powder particle size and the spray distance. The smaller the particle size, and the shorter the spray distance, the denser the microstructure. Early work had shown that the thermal conductivity of a typical EB-PVD TBC is somewhat greater than that of plasma sprayed TBCs (Nagaraj, 1988). This was attributed to the greater horizontal porosity in the plasma sprayed coatings. Within the plasma sprayed TBCs, a denser coating (typically used on thicker coatings for shroud or combustor applications) has a higher thermal conductivity than a porous coating (typically used on thinner coatings for airfoil applications). Using the measured thermal conductivity, the temperature reduction was estimated to be 38-66°C (100-150°F) for a 127 micrometer (5 mil.) thick EB-PVD TBC on the stage 1 high pressure turbine blade of a high by-pass engine. The measured temperature reduction (using the standard gamma prime volume percent in the alloy) in a factory engine test was in rough agreement with the calculated value.

EXPERIMENTAL TECHNIQUE

Determining thermal conductivity from diffusivity data is preferred over direct steady-state thermal conductivity measurements at high temperatures. This is particularly true for low conductivity materials and when only small volumes of material are available. Such is the case with thermal barrier coatings. Thermal conductivity values were calculated from the relationship $\mathbf{k}=\alpha\rho C_p$, where $\mathbf{k}$ is the thermal conductivity, α is the thermal diffusivity, ρ is the bulk density, and C_p is the specific heat at constant pressure. Specific heat measurements were made by Differential Scanning Calorimeter (DSC).

Thermal diffusivity measurements were made at room temperature in air using the xenon flash diffusivity system located at the High Temperature Materials Laboratory (HTML) at Oak Ridge National Laboratory (ORNL). High temperature measurements were made in vacuum ($<10^{-5}$ Torr) using the laser flash thermal diffusivity system also located at the HTML at ORNL (see Fig. 5). The laser is a 50 Joule, neodymium/glass laser with a wavelength of 1.06 µm and a pulse width of 0.6 ms. The laser is operated at a low power to limit the temperature rise of the rear surface of the test specimen to less than 3°C. Both the room temperature and high temperature systems use an InSb infrared detector to monitor the relative temperature rise of the rear surface of the test specimen. The detector output is recorded as a function of time by an analog-to-digital converter and computer. The data for free standing coatings are analyzed using the Koski (1981) parameter estimation algorithm, Clark and Taylor (1975) heat loss corrections and the Heckman (1973) finite pulse width correction. The free standing EB-PVD specimens are very fragile since they are typically 127-203 micrometers (5-8 mil.) thick.. Thus, most of the EB-PVD specimens are measured on a 500 micrometer (20 mil.) thick nickel foil using the 2-layer data analysis techniques of Lee and Taylor (1974).

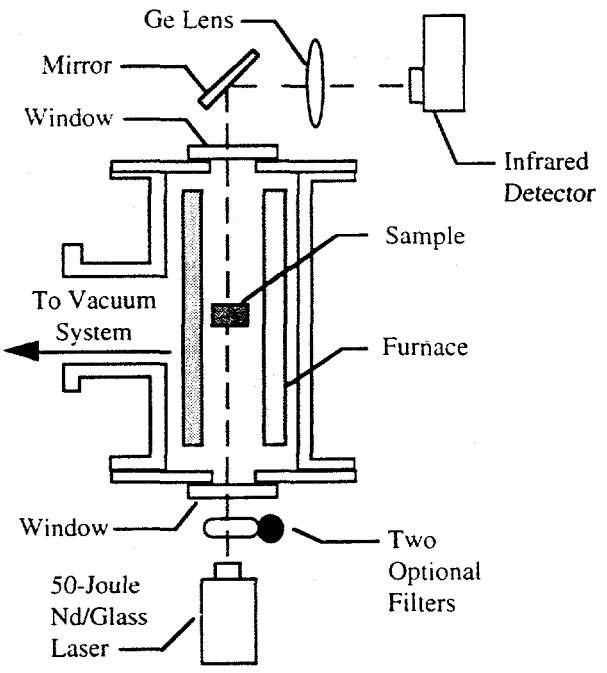

Fig. 5. Laser Flash Thermal Diffusivity System.

RESULTS AND DISCUSSION

The specific heats of PVD and plasma sprayed TBCs were found (see Fig. 6) to be in excellent agreement with calculated values obtained by taking the mass weighted average of literature values for ZrO_2 (Coughlin and King, 1950) and Y_2O_3 (Pankratz et al., 1962). The curve in Fig. 6 was generated from a non-linear least squares fit of the Equation

$$C_p = \frac{1}{\left(A_1 T^{A_2} + \frac{A_3}{T^{A_4}}\right)} \qquad (1)$$

T is the absolute temperature in Kelvin, Cp is the specific heat in units of J/Kg K, and A_1, A_2, A_3, and A_4 are fitting parameters. These values are: A_1=0.00345, A_2=-0.1088, A_3=2727.03, and A_4=2.7832.

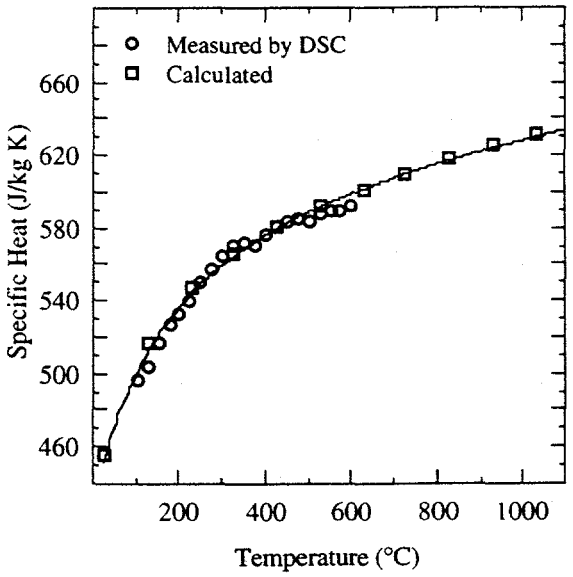

Fig. 6. Specific Heat of Yttria-PSZ.

Both high and low density yttria-PSZ coatings were manufactured using the APS deposition technique. The density of a coating can be controlled by varying the spray parameters such as spray distance, powder size, dwell time, etc. The thermal conductivity of these APS coatings were measured as a function of temperature and compared to the thermal conductivity of yttria-PSZ coatings made by the EB-PVD technique. The results are shown in Fig. 7. The thermal conductivity of 97% dense yttria-PSZ is shown for comparison (Mirkovich, 1976). The thermal conductivity of the EB-PVD coating is significantly higher than the APS coatings. This difference is not due solely to differences in density since the densities of the EB-PVD specimen (5.1 g/cm^3) is comparable to that of the high density APS specimen (5.3 g/cm^3). The density of fully dense yttria-PSZ is 6.05 g/cm^3 (Brandt, et al., 1986). The fact that the high density APS coating has a lower thermal conductivity than the EB-PVD coating is primarily due to the morphology of the porosity. The porosity at the splat boundaries is oriented with its major axis perpendicular to the heat flow and thus is a much better barrier to the heat flow than spherical pores. Conversely, the porosity in the EB-PVD coating is oriented with its major axis parallel to the heat flow and thus has relatively little effect on the heat flow. Comparing the APS coatings we see that decreasing the density from 5.3 g/cm^3 down to 4.7 g/cm^3 has a significant effect on lowering the thermal conductivity. This difference is largest at room temperature, but is still approximately 25% at 1000°C.

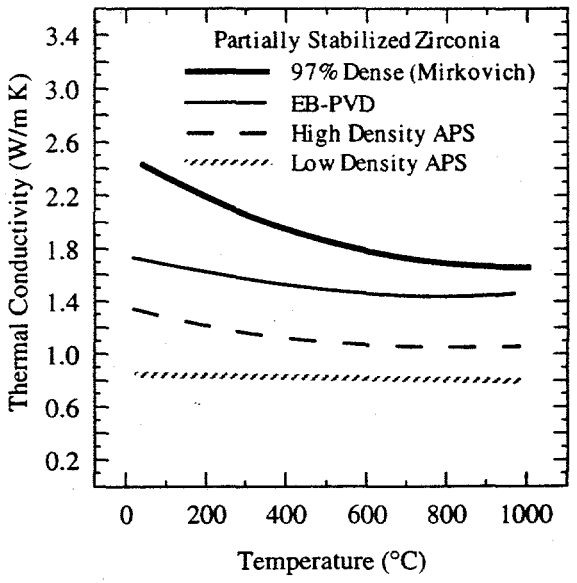

Fig 7. The Effect of Deposition Technique on the Thermal Conductivity of Yttria-PSZ

Five low density yttria-PSZ coatings were manufactured to study the effect of high temperature heat treatments on the room temperature thermal conductivity. One specimen remained untreated as a control while the other four specimens were isothermally heat treated for 1000 hours each at temperatures in the range 871°C to 1371°C (1600°F to 2500°F). The thermal conductivity was determined for each specimen at 20°C in air. The results are shown in Fig. 8. The 5% difference between the normalized thermal conductivity of the specimen heat treated at 871°C and the untreated specimen is within the experimental error of the measurement. However, there is a large increase in the thermal conductivity of the specimen heat treated at 1038°C (1900°F). The thermal conductivity continues to increase as the heat treatment temperature increases.

This irreversible increase in the thermal conductivity of plasma sprayed structures has been previously reported for yttria fully stabilized zirconia (Wilkes and Lagedrost, 1973, and Eaton et al., 1994), yttria-PSZ (Taylor, 1992), as well as zirconia stabilized with other oxides, such as CaO (Wilkes and Lagedrost, 1973, and Brandt, 1981), and CeO_2 (Brandon and Taylor, 1989). This effect has also been reported for plasma sprayed Al_2O_3, yttria-stabilized HfO_2, and Mo (Wilkes and Lagedrost, 1973). The increase in thermal conductivity is due to sintering of the splat structure of the coating. As the coating begins to sinter, necking is observed between the splats, enhancing the heat flow from splat to splat. Finally, the morphology of the porosity changes from plate-like at the splat boundaries to chains of small spherical pores within a continuous structure (Eaton, et al., 1994). During this sintering process the overall bulk density of the coating changes very little. However, the morphology changes in the porosity have a significant effect in increasing the heat flow within the coating and hence its thermal conductivity.

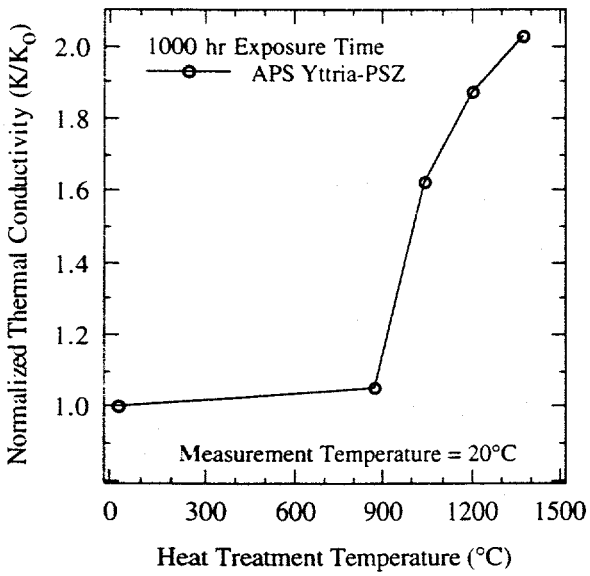

Fig 8. The Effect of Heat Treatment Temperature on the Room Temperature Thermal Conductivity of APS Yttria-PSZ.

Figure 9 illustrates the effect of heat treatment time on the thermal conductivity of yttria-PSZ manufactured using the EB-PVD process. The coatings were deposited on nickel foil without a bondcoat. Specimens were isothermally heat treated, in an inert gas, at various times from 1 hour to 70 hours at 1038°C (1900°F). One specimen was left untreated as a control. The thermal conductivity was determined at 20°C using two-layer analysis as described by Lee and Taylor (1974). Since this type of analysis requires knowledge of the thickness, density, specific heat, and thermal diffusivity of the substrate as well as of the coating, the absolute accuracy is expected to be lower than in the case of free standing coatings used in the other measurements described in this paper. However, the relative changes in thermal conductivity are expected to be valid since only the thermal conductivity of the coating is changing between specimens. Figure 9 shows that the thermal conductivity increases with increasing heat treatment time. However, the rate of this change decreases with time. Nearly half of the total observed increase occurs in the first 7 hours (0.1 of the total heat treatment time). The thermal conductivity of the specimen heat treated for 70 hours is approximately 10% greater than the untreated specimen.

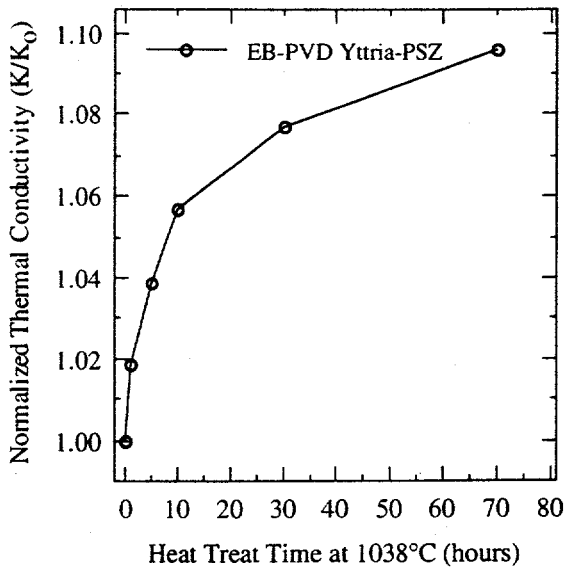

Fig. 9. The Effect of Heat Treatment Time at 1038°C on the Room Temperature Thermal Conductivity of EB-PVD Yttria-PSZ.

A set of EB-PVD yttria-PSZ coatings were cyclically heat treated to 1135°C (2075°F). Each cycle consisted of heating the specimen to 1135°C for 45 minutes and then cooled to room temperature. The room temperature (20°C, 68°F) thermal conductivity of each coating was determined before and after heat treatments. These were relatively thick, approximately 625 micrometers (approximately 25 mil.), EB-PVD TBCs, and free standing coatings were used for the thermal diffusivity measurements. The number of cycles ranged from 440 to 620 with one specimen left untreated as a control. Figure 10 shows the fractional increase in room temperature thermal conductivity as a function of the number of heat treatment cycles to 1135°C

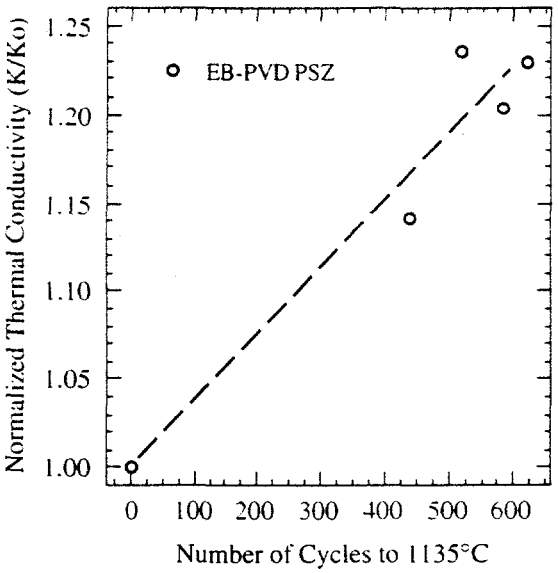

Fig. 10. The Fractional Increase in Room Temperature Thermal Conductivity of EB-PVD Deposited Yttria-PSZ as a Function of the Number of Cycles from 20°C to 1135°C.

(2075°F). There is a general increase in the normalized thermal conductivity with the number of cycles up to a maximum observed increase of about 23%.

We can use the Larson-Miller parameter approach described by Eaton et. al. (1994) to compare the thermal conductivity data of coatings heat treated at different times and temperatures. The Larson-Miller parameter combines both the heat treatment time (seconds) and temperature (Kelvin) in such a way as to result in a linear relationship when plotted against the natural log of the normalized thermal conductivity. The Larson-Miller parameter, L-M, is calculated from Eq. 2,

$$LM = T\,[\ln(t) + 80] \qquad (2)$$

where T is the absolute temperature in Kelvin, and t is the time, in seconds, at temperature. The slope of the resulting lines represents the susceptibility of a coating to thermal aging effects. The greater the slope, the greater the increase in thermal conductivity for a given set of heat treatment parameters. Figure 11 shows the Larson-Miller plot for APS yttria-PSZ and EB-PVD yttria-PSZ. Previous results for APS yttria-FSZ (porosity range 6.7 to 32%) are also shown for comparison (Eaton et al., 1994). This figure shows that the partially stabilized coatings are less susceptible to thermal aging compared to the fully stabilized coatings. The yttria fully stabilized zirconia has a much lower thermal conductivity than partially stabilized zirconia (Brandt et al., 1986), but this conductivity increases faster than PSZ above 1000°C. The reason why FSZ APS coatings would behave differently from PSZ APS coatings is currently under study.

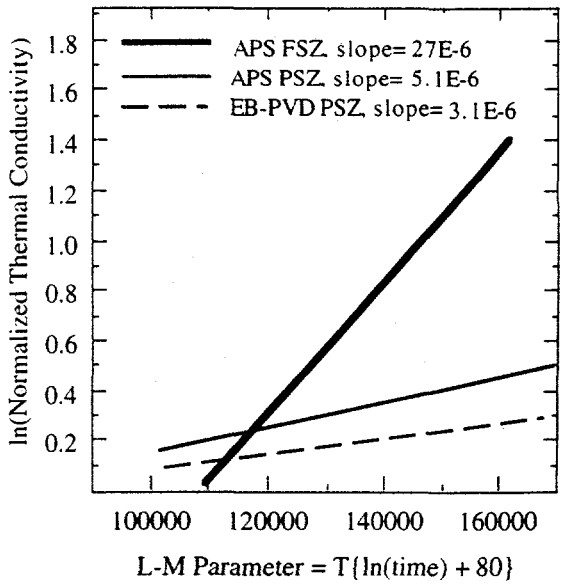

Fig. 11. Normalized Thermal Conductivity as a Function of Larson-Miller Parameter for APS Partially and Fully Stabilized Zirconia and EB-PVD PSZ.

CONCLUSIONS

The effect of high temperature isothermal heat treatments on partially yttria stabilized zirconia TBCs deposited by both APS and EB-PVD techniques have been studied. These results have been compared with previous results for fully yttria stabilized zirconia. Low density APS yttria-PSZ coatings have a lower thermal conductivity than high density APS yttria-PSZ coatings. After thermal aging (T > 1000 °C), the thermal conductivity of APS coatings increased substantially. However, APS yttria-FSZ exhibits larger increases in thermal conductivity due to thermal aging than APS yttria-PSZ. EB-PVD PSZ coatings posses a higher thermal conductivity than APS coatings, before heat treatments. However, EB-PVD yttria-PSZ coatings are less susceptible to the effects of thermal aging than either APS yttria-PSZ or APS yttria-FSZ. Generally, for yttria stabilized zirconia, the lower the as-fabricated thermal conductivity, the more susceptible that coating is to increases in thermal conductivity due to thermal aging above 1000°C. If these coatings reach a temperature above 1000°C during operation, they will begin to lose some of their effectiveness as a thermal barrier.

ACKNOWLEDGMENTS

The authors wish to thank Chad S. Moore for making many of the thermal diffusivity measurements at HTML and Karren L. More, of ORNL, for the SEM micrographs. The authors wish to thank W. Nelson, A. Maricocchi, R. Zimmerman, and M. Schmidt (all of General Electric) for their help with the preparation and thermal exposure of the specimens. Research sponsored by the U.S. Department of Energy, Assistant Secretary for Energy Efficiency and Renewable Energy, Office of Transportation Technologies, as part of the High Temperature Materials Laboratory User and Fellowship Programs, under contract DE-AC05-96OR22464 managed by Lockheed Martin Energy Research Corporation.

REFERENCES

Brandon, J. R. and Taylor, R., 1989, "Thermal Properties of Ceria and Yttria Partially Stabilized Zirconia Thermal Barrier Coatings," Surface and Coating Technology, 39/40 p143-51.

Brandt, R., 1981, "Thermal Diffusivity Measurements on Plasma-Sprayed CaO-Stabilized ZrO_2," High Temperature-High Pressure, vol. 13, p79-88.

Brandt, R., Pawlowski, L. and Neuer, G., 1986, "Specific Heat and Thermal Conductivity of Plasma Sprayed Yttria-Stabilized Zirconia and NiAl, NiCr, NiCrAl, NiCrAlY, NiCoCrAlY coatings," High Temperature-High Pressure, vol. 18, p65-77.

Clark, L. M. and Taylor, R. E., 1975, "Radiation Loss in the Flash Method for Thermal Conductivity," Journal of Applied Physics, vol. 46, No. 2, pp714-19.

Coughlin, J. P. and King, E. G., 1950, Journal of the American Chemical Society, vol. 72, pp2262-5, as tabulated in Touloukian, Y. S. , and E. H. Buyco, 1970, "Specific Heat of Nonmetallic Solids," Thermophysical Properties of Matter, vol. 5, IFI/Plenum, NY.

Eaton, H. E., Linsey, J. R. and Dinwiddie, R. B., 1994, "The Effect of Thermal Aging on the Thermal Conductivity of Plasma Sprayed Fully Stabilized Zirconia," pp. 289-300 in Thermal Conductivity 22, ed. T. W. Tong, Technomic Pub. Co. Inc., Lancaster PA.

Heckman, R. C., 1973, "Finite Pulse-Time and Heat Loss Effects in Pulsed Thermal Diffusivity Measurements," Journal of Applied Physics, vol. 44, No. 4, pp1455-61.

Koski, A., 1981, "Improved Data Reduction Methods for Laser Pulse Diffusivity Determination with the Use of Minicomputers," pp. 94-103 in *Proceedings of the Eighth Symposium on Thermophysical Properties*, vol. 2, ed. Jan V. Sengers, The American Institute of Physics

Lee, H. J. and Taylor, R. E., 1974, "Determination of Thermophysical Properties of Layered Composites by Flash Method," Thermal Conductivity 14, Eds. P. G. Klemens and L. K. Chu, Plenum Pub. Corp., NY, pp423-434.

Maricocchi, A. F., Bartz, A. and Wortman, D. J., 1995, "PVD TBC Experience on GE Aircraft Engines," Proc. NASA TBC Workshop. held in Cleveland Ohio, March 27-29, NASA Conf. Pub. 3312, pp79-83.

Meier, S. M. and Gupta, D. K., 1992, "The Evolution of Thermal Barrier Coatings in Gas Turbine Engine Application," ASME Conf. Publication, 92-GT-203.

Mirkovich, V. V., 1976, "Thermal Diffusivity of Yttria-Stabilized Zirconia," High Temperature-High Pressure, vol. 8, pp231-35.

Nagaraj, B. A. and Nelson, W. A., Unpublished Work, 1988.

Pankratz, L. B., King, E. G. and Kelly, 1962, U.S. Bur. Mines, Report Investigation 6033, pp1-18, as tabulated in Touloukian, Y. S. , and E. H. Buyco, 1970, "Specific Heat of Nonmetallic Solids," Thermophysical Properties of Matter, vol. 5, IFI/Plenum, NY.

Taylor, T. A., 1992, "Thermal Properties and Microstructure of Two Thermal Barrier Coatings," Surface and Coating Technology, vol. 54, pp53-7

Wilkes, K. E. and Lagedrost, J. F., 1973, "Thermophysical Properties of Plasma Sprayed Coatings," NASA CR-121144, under contract NAS3-13329.

Wortman, D. J., Nagaraj, B. A. and Duderstadt, E. C., 1989, "Thermal Barrier Coatings for Gas Turbine Use," Materials Science and Engineering, A121, pp 433-440.